

**Variability in surface ozone background over the United States:  
Implications for air quality policy**

A. Fiore, D. Jacob, H. Liu<sup>1</sup>, R.M. Yantosca, T.D. Fairlie<sup>1</sup>, Q. Li

Department of Earth and Planetary Sciences and Division of Engineering and Applied Sciences,  
Harvard University, Cambridge, MA

<sup>1</sup>Now at National Institute of Aerospace, Hampton, VA

Short Title: Variability in U.S. surface O<sub>3</sub> background

Submitted to *J. Geophys. Res.*, June 12, 2003

## Abstract

The U.S. Environmental Protection Agency (EPA) presently uses a 40 ppbv background O<sub>3</sub> level as a baseline in its O<sub>3</sub> risk assessments. This background is defined as those concentrations that would exist in the absence of North American emissions. *Lefohn et al.* [2001] have argued that frequent occurrences of O<sub>3</sub> concentrations above 50-60 ppbv at remote northern U.S. sites in spring are of stratospheric origin, challenging the EPA background estimate and implying that the current O<sub>3</sub> standard (84 ppbv, 8-hour average) may be unattainable. We show that a 3-D global model of tropospheric chemistry reproduces much of the observed variability in U.S. surface O<sub>3</sub> concentrations, including the springtime high-O<sub>3</sub> events, with only a minor stratospheric contribution (always < 20 ppbv). We conclude that the previous interpretations of a stratospheric source for these events underestimated the role of regional and hemispheric pollution. While stratospheric intrusions might occasionally elevate surface O<sub>3</sub> at high-altitude sites, our results indicate that these events are rare and would not compromise the O<sub>3</sub> air quality standard. We find that the O<sub>3</sub> background is generally 15-35 ppbv, with some incidences of 40-50 ppbv in the west in spring at high-elevation sites (> 2 km). It declines from spring to summer and further decreases during O<sub>3</sub> pollution episodes. The 40 ppbv background assumed by EPA thus actually underestimates the risk associated with O<sub>3</sub> during polluted conditions. A better definition would represent background as a function of season, altitude, and total surface O<sub>3</sub> concentration. Natural O<sub>3</sub> levels are typically 10-25 ppbv and never exceed 40 ppbv. International controls to reduce the hemispheric pollution background would facilitate compliance with an AOT40-type standard (cumulative exposure to O<sub>3</sub> above 40 ppbv) in the United States.

## 1. Introduction

When setting the national ambient air quality standard (NAAQS) for ozone (O<sub>3</sub>) in surface air over the United States, the U.S. Environmental Protection Agency (EPA) accounts for a background O<sub>3</sub> level above which risk to human health is assessed. Since there is no known “safe” threshold of O<sub>3</sub> associated with negligible risk [*McDonnell et al.*, 1993], the EPA calculates the marginal risk from O<sub>3</sub> concentrations above the background. The exact specification of the background thus has important implications for risk assessments. In theory, the background should represent natural concentrations of O<sub>3</sub>, but it is well established that

human activities enhance O<sub>3</sub> throughout the northern hemispheric troposphere [Marenco *et al.*, 1994; Kasibhatla *et al.*, 1996]. In practice, the EPA defines as background the O<sub>3</sub> concentrations that would exist in the absence of North American anthropogenic emissions, i.e., O<sub>3</sub> that is not amenable to reduction via domestic emission controls [U.S. EPA, 2003]. We apply here a global 3-D chemical transport model (CTM) to quantify this background and its variability, and to separate the natural background from the enhancement due to hemispheric pollution. We find that the traditional approach for estimating background O<sub>3</sub> from measurements at remote sites underestimates the contribution from regional and hemispheric pollution, yielding erroneously high values for the natural background.

Ozone is produced in the troposphere when volatile organic compounds (VOC) and carbon monoxide (CO) are photochemically oxidized in the presence of nitrogen oxides (NO<sub>x</sub>). It is also transported to the troposphere from the stratosphere. The NO<sub>x</sub>, VOC and CO precursors of O<sub>3</sub> have anthropogenic sources including fuel combustion and biomass burning, as well as natural sources including lightning, wildfires, soils and vegetation. In polluted regions such as the eastern United States, anthropogenic emissions of NO<sub>x</sub>, VOC and CO lead to high-O<sub>3</sub> episodes endangering public health. In the remote troposphere, O<sub>3</sub> is generally thought to be in approximate steady-state between chemical sources and sinks that are much larger than the contribution from the stratosphere [Prather and Ehhalt, 2001].

The standard approach used by EPA to estimate background O<sub>3</sub> levels in the United States has been based on simple observational statistics. Specific approaches have included analyses of O<sub>3</sub> probability distributions, measurements at remote sites, and correlations with tracers of regional pollution (Table 1). On the basis of these studies, the EPA chose a 25-45 ppbv range to encompass the variations in background levels for daytime hours from April to October over the United States [U.S. EPA, 1996a] and then adopted a 40 ppbv level for use in risk assessments [U.S. EPA, 1996b]. This background range was instrumental in setting the current NAAQS for O<sub>3</sub>: an 8-hour mean concentration of 84 ppbv not to be exceeded more than three times per year for a three year averaging period. Results from modeling studies where the background is estimated by zeroing anthropogenic emissions in North America (Table 1) are on the low end of the 25-45 ppbv range, suggesting that the 40 ppbv background used in EPA risk assessments is too high.

A recent study by *Lefohn et al.* [2001] has challenged the EPA's definition of background and suggests that compliance with the current NAAQS for O<sub>3</sub> may be unachievable due to high natural background levels. These authors found that hourly O<sub>3</sub> concentrations measured at remote northern U.S. sites in spring are often in the 40-80 ppbv range, with frequent occurrences above 50 and 60 ppbv. They argue that these observations represent natural background O<sub>3</sub> levels with a substantial stratospheric component, and imply that the natural background may be similarly high across the country. If their analysis is correct, it would follow that (1) the present standard as well as any lower future standard may be unattainable and (2) the 40 ppbv background used in the EPA risk assessments is too low.

We show below that our global CTM can simulate the high-O<sub>3</sub> events at remote U.S. sites as reported by *Lefohn et al.* [2001]. We analyze the CTM results to gain insight into the origin of these events. We find that they can generally be explained by regional pollution, with some contribution from hemispheric pollution. The natural background never exceeds 40 ppbv.

## **2. The GEOS-CHEM Model**

### **2.1. Model Description**

We apply the GEOS-CHEM CTM (version 4.33; <http://www-as.harvard.edu/chemistry/trop/geos/index.html>) to a simulation of global tropospheric O<sub>3</sub>-NO<sub>x</sub>-hydrocarbon chemistry for 2001. The model uses assimilated meteorological data from the NASA Goddard Earth Observing System (GEOS-3) at 1° x 1° horizontal resolution with 48 vertical layers. We regrid the meteorological fields to 2° x 2.5° horizontal resolution and retain the original vertical resolution. The temporal resolution of the meteorological data is 3 hours for mixing depths and surface variables and 6 hours for winds, convective mass fluxes, and other three-dimensional variables. The GEOS-CHEM NO<sub>x</sub> emissions for 2001 from fuel combustion, excluding aircraft, are 25.6 Tg N yr<sup>-1</sup> globally and 6.3 Tg N yr<sup>-1</sup> for the United States. The latter value is consistent with estimates from *U.S. EPA* [2002]. Additional global emissions of NO<sub>x</sub> in the model include 6.5 Tg N yr<sup>-1</sup> from biomass burning, 5.3 Tg N yr<sup>-1</sup> from natural soil emissions, 4.7 Tg N yr<sup>-1</sup> from lightning, and 0.5 Tg N yr<sup>-1</sup> each from fertilizer application and aircraft. We impose a uniform global CH<sub>4</sub> concentration of 1750 ppbv, based upon observations for 2000 [*Prather and Ehhalt*, 2001]. Global natural emissions of isoprene and monoterpenes in the model for 2001 are 340 Tg C yr<sup>-1</sup> and 130 Tg C yr<sup>-1</sup>, respectively. The isoprene emission

inventory for the United States is discussed in detail by *Palmer et al.* [2003]. Further details of the GEOS-CHEM model version used here are given in *Evans et al.* [2003].

GEOS-CHEM applies the Synoz method [*McLinden et al.*, 2000] to impose a net global  $\text{O}_3$  flux of  $490 \text{ Tg O}_3 \text{ yr}^{-1}$  from the stratosphere to the troposphere. This flux is consistent with the  $475 \pm 120 \text{ Tg O}_3 \text{ yr}^{-1}$  range constrained by observations [*McLinden et al.*, 2000]. Ozonesonde climatologies for extratropical latitudes provide a test of the simulation of stratospheric influence on tropospheric  $\text{O}_3$  [*Logan*, 1999]. *Bey et al.* [2001a] showed that GEOS-CHEM simulates the tropospheric ozonesonde climatology generally to within 10 ppbv, including at mid and high northern latitudes in winter, and reproduces the phase of the seasonal cycle to within 1-2 months. *Li et al.* [2002a] demonstrated that GEOS-CHEM reproduces the springtime ozonesonde observations over Bermuda and North America to within 5 ppbv. *Liu et al.* [2002] further showed a successful GEOS-CHEM simulation of the ozonesonde climatology from sites along the Asian Pacific rim. A more recent analysis of the  $^{210}\text{Pb}$ - $^7\text{Be}$ - $\text{O}_3$  relationships observed in three aircraft missions over the western Pacific suggests that the model does not underestimate the stratospheric source of  $\text{O}_3$  [*Liu et al.*, 2003a]. These studies and others [*Li et al.*, 2001; *Bey et al.*, 2001b; *Fusco and Logan*, 2003] demonstrate that the model provides an adequate simulation of  $\text{O}_3$  in the free troposphere at northern midlatitudes, including the influence from the stratosphere.

Several GEOS-CHEM studies have focused on North America and presented evaluations with observations from surface sites, aircraft, and satellites. They have addressed issues of chemical outflow of  $\text{O}_3$ , CO, and  $\text{NO}_y$  to the Atlantic [*Li et al.*, 2002ab, 2003], long-term CO trends [*Duncan et al.*, 2003], sources of carbonaceous aerosols [*Park et al.*, 2003], and current U.S. emissions inventories of isoprene and  $\text{NO}_x$  [*Palmer et al.*, 2001, 2003; *Martin et al.*, 2003]. Of particular relevance for this study, the model has been used to examine the role of background  $\text{O}_3$  on U.S. air quality [*Fiore et al.*, 2002a].

*Fiore et al.* [2002a, 2003] presented a detailed evaluation of the model simulation for  $\text{O}_3$  and related species over the United States for the summer of 1995. They showed that the model reproduces important features of observations including the high tail of  $\text{O}_3$  frequency distributions at sites in the eastern United States (although sub-grid scale local peaks are underestimated), the  $\text{O}_3$ : [ $\text{NO}_y - \text{NO}_x$ ] relationships, and the “piston effect” (the highest  $\text{O}_3$  values exhibit the largest response to decreases in U.S. fossil fuel emissions from 1980 to 1995)

[Lefohn *et al.* 1998]. Empirical orthogonal functions (EOFs) for the observed regional variability of O<sub>3</sub> over the eastern United States are also well reproduced, indicating that GEOS-CHEM captures the synoptic-scale transport processes modulating surface O<sub>3</sub> concentrations [Fiore *et al.*, 2003]. Model shortcomings relevant for this study include: (1) an overestimate in urban coastal environments due to inadequate resolution of the gradient in mixing depths across coastlines, (2) excessive convective mixing over the Gulf of Mexico and the Caribbean which leads to an overestimate of O<sub>3</sub> concentrations in southerly flow over the southeastern United States. Comparison of GEOS-CHEM with the Multiscale Air Quality Simulation Platform (MAQSIP) regional air quality modeling system [Odman and Ingram, 1996] at 36 km<sup>2</sup> horizontal resolution showed that the models exhibit similar skill at capturing the observed variance in O<sub>3</sub> concentrations, with comparable model biases [Fiore *et al.*, 2003].

## 2.2 Simulations

We quantify the sources contributing to the O<sub>3</sub> background over the United States with three simulations: (1) a standard simulation, (2) a background simulation in which North American anthropogenic NO<sub>x</sub>, NMVOC and CO emissions are set to zero, and (3) a natural O<sub>3</sub> simulation in which global anthropogenic NO<sub>x</sub>, NMVOC and CO emissions are set to zero and the CH<sub>4</sub> concentration is set to its 700 ppbv pre-industrial value. Anthropogenic emissions of NO<sub>x</sub>, NMVOC, and CO include contributions from fuel use, industry, and fertilizer application. A tagged O<sub>3</sub> tracer simulation [Fiore *et al.*, 2002a] is used to isolate the stratospheric contribution to the background and yields results that are quantitatively consistent with those from a simulation in which O<sub>3</sub> transport from the stratosphere to the troposphere is suppressed [Fusco and Logan, 2003]. Table 2 summarizes the simulations used for source attribution. The difference between the standard and background simulations represents regional pollution, i.e., the O<sub>3</sub> enhancement from North American anthropogenic emissions. The difference between the background and natural simulations represents hemispheric pollution, i.e., the O<sub>3</sub> enhancement from anthropogenic emissions outside North America. Methane and NO<sub>x</sub> contribute most to hemispheric pollution [Fiore *et al.*, 2002b]. All simulations were initialized in June 2000; we report results for March through October 2001.

The standard and background simulations are conducted at 2° x 2.5° horizontal resolution but the natural simulation is conducted at 4° x 5° resolution to save on computational time.

From our past experience (e.g. *Fiore et al.* [2002a]), there should be no significant bias between  $4^\circ \times 5^\circ$  and  $2^\circ \times 2.5^\circ$  simulations, particularly for a natural  $O_3$  simulation where concentrations are controlled by large-scale processes. We will also show results from a  $4^\circ \times 5^\circ$  tagged  $O_3$  tracer simulation for 2000 for comparison with an observed time series in North Carolina.

### 3. Mean Background Concentrations: Spatial and Seasonal Variation

Our analysis focuses on the 2001 observations from the Clean Air Status and Trends Network (CASTNet) of rural and remote U.S. sites [*Lavery et al.*, 2002] (Figure 1). In Figure 2, we present the mean seasonal cycle in afternoon (13-17 local time (LT))  $O_3$  concentrations averaged over the CASTNet stations in each U.S. quadrant. Measured  $O_3$  concentrations (black asterisks) are highest in April-May, except in the northeast where they peak in June. Model results (red triangles) are within 2 ppbv of the observations for all months in the northwest. Agreement in the southwest is also generally good but the observed May maximum is underestimated by 5 ppbv. Model results for the northeast are too high by 5-8 ppbv when sampled at the CASTNet sites; the model is lower when we sample the ensemble of grid squares in the region (red squares). The model is 10 ppbv too high over the southeast in summer for reasons discussed in section 2.1.

Results from the background simulation (no anthropogenic emissions in North America; see Table 2) are shown as green diamonds in Figure 2. Mean background  $O_3$  ranges from 20 ppbv in the northeast in summer to 35 ppbv in the northwest in spring. It is higher in the west than in the east because of higher elevation, deeper mixed layers, and longer  $O_3$  lifetimes due to the arid climate [*Fiore et al.*, 2002a]. It is also higher in spring than in summer, in part because of the seasonal maximum of stratospheric influence (Figure 2) and in part because of the longer lifetime of  $O_3$  [*Wang et al.*, 1998].

Results from the natural  $O_3$  simulation (no anthropogenic emissions anywhere; Table 2) are shown as blue crosses in Figure 2. Similar to the background, natural  $O_3$  concentrations are highest in the west in spring. The ranges in the monthly mean natural  $O_3$  concentrations are 18-23, 18-27, 13-20, and 15-21 ppbv in the northwest, southwest, northeast, and southeast, respectively. Values are highest in spring when the influence of stratospheric  $O_3$  on the troposphere peaks [e.g. *Holton et al.*, 1995]. The stratospheric contribution (blue X's) ranges from 7 ppbv in spring to 2 ppbv in summer.

The difference between the background and natural simulations in Figure 2 represents the monthly mean hemispheric pollution enhancement. This enhancement ranges from 5 to 12 ppbv depending on region and season. It peaks in spring due to a longer O<sub>3</sub> lifetime [Wang *et al.*, 1998] and more efficient ventilation of pollution from the Asian continent [Liu *et al.*, 2003b]. In contrast to hemispheric pollution, the regional pollution influence (difference between the red squares and green diamonds) peaks in summer (June for the northern quadrants, July for the southern quadrants) and is highest in the east. For the data in Figure 2 it ranges from 8 ppbv in the northern quadrants in March to over 30 ppbv in the eastern quadrants in summer. We conclude that monthly mean observed O<sub>3</sub> concentrations are influenced by both regional and hemispheric pollution in all U.S. regions from March through October and that the higher background in spring reflects coincident spring maxima in the contributions from hemispheric pollution and stratospheric influence, as previously pointed out by Wang *et al.* [1998].

#### 4. Frequency of High-O<sub>3</sub> Occurrences at Remote Sites

Lefohn *et al.* [2001] pointed out the frequent occurrence of high-O<sub>3</sub> events ( $\geq 50$  and 60 ppbv) at remote northern U.S. sites in spring. In this section, we calculate the frequency of these events in the CASTNet data for 2001, determine whether 2001 is a representative year, and then assess the ability of the model to reproduce these events. We first replicate the analysis of Lefohn *et al.* [2001] at the four CASTNet sites that they examined: Denali National Park (Alaska), Voyageurs National Park (Minnesota), Glacier National Park (Montana), and Yellowstone National Park (Wyoming). We calculate the number of times that the hourly O<sub>3</sub> observations at the sites are  $\geq 50$  and 60 ppbv for each month from March to October 2001. Results are shown in Table 3. Comparison with the same statistics for March through June 1988-1998 in Tables 2 and 3 of Lefohn *et al.* [2001] enables us to place the 2001 statistics in the context of other years. More incidences of O<sub>3</sub> above both thresholds occur at Denali National Park (NP) and Yellowstone NP in 2001 than in nearly all of the years analyzed by Lefohn *et al.* [2001]. The statistics at Glacier NP, Montana, indicate that 2001 had fewer than average incidences of high-O<sub>3</sub> events. At Voyageurs NP in Minnesota, March and April 2001 had lower-than-average frequencies of high-O<sub>3</sub> events but May and June were more typical. Overall, we consider 2001 to be a suitable year for analysis of high-O<sub>3</sub> events.



If we consider all CASTNet sites, we find that O<sub>3</sub> concentrations  $\geq 70$  and 80 ppbv occur most often in May through August (not shown). These events are clearly associated with regional pollution as shown in sections 6 and 7.

We wish to use the GEOS-CHEM model to interpret the origin of the high-O<sub>3</sub> events in the CASTNet observations. As pointed out by *Fiore et al.* [2002a], comparison of model results with surface observations is most appropriate in the afternoon when the observations are representative of a relatively deep mixed layer. In addition, the model does not provide independent information on an hour-to-hour basis since it is driven by meteorological fields that are updated every six hours. In *Fiore et al.* [2002a] we used mean 13-17 LT surface observations for model evaluation, and we test here whether an analysis restricted to these mean afternoon concentrations captures the same frequency of O<sub>3</sub>  $\geq 50$  and 60 ppbv that emerges from an analysis of the individual hourly concentrations. Results in Table 3 show that the percentage of individual afternoon (13-17 LT) hours when O<sub>3</sub>  $\geq 50$  and 60 ppbv at the CASTNet sites is always greater than the percentage of all hourly occurrences above these thresholds, indicating that elevated O<sub>3</sub> concentrations preferentially occur in the afternoon. Furthermore, we see from Table 3 that the frequency of observation of high-O<sub>3</sub> events is not diminished when 4-hour average (13-17 LT) concentrations are considered, reflecting persistence in the duration of these events. Model frequencies of high-O<sub>3</sub> events from 13-17 LT at the CASTNet sites are similar to observations in spring, as shown in Table 3, and about 10% higher in the summer largely because of the positive model bias in the southeast discussed in section 2.

## 5. Natural vs. Anthropogenic Contributions to the High-O<sub>3</sub> occurrences

Figure 3 shows probability distributions constructed from the ensemble of daily mean afternoon (13-17 LT) O<sub>3</sub> concentrations in surface air at the CASTNet sites for March through October 2001. Model distributions for background, natural, and stratospheric O<sub>3</sub> (Table 2) are also shown. The success of the model in capturing the overall distribution of the observed concentrations provides confidence that it can adequately describe the ranges in the background and its sources.

The background (long-dashed green line) ranges from 10 to 50 ppbv with most values in the 20-35 ppbv range. This result implies that health risks from O<sub>3</sub> exposure are underestimated by the assumption of a 40 ppbv background in EPA risk assessments. The full 10-50 ppbv range

of background predicted here encompasses the previous 25-45 ppbv estimates shown in Table 1. However, background estimates from observations tend to be at the higher end of the range (25-45 ppbv) while our results as well as those from prior modeling studies (Table 1) indicate that background concentrations in surface air are usually below 40 ppbv. The background concentrations derived from observations could be overestimated if observations at remote and rural sites contain some influence from regional pollution (as shown below to occur in the model), or if the  $O_3$  vs.  $NO_y$ - $NO_x$  correlation is affected by different relative removal rates of  $O_3$  and  $NO_y$  [Trainer *et al.*, 1993].

We find that natural  $O_3$  concentrations (short-dashed light blue line) are generally in the 10-25 ppbv range and never exceed 40 ppbv. The range of the hemispheric pollution enhancement (the difference between the background and natural  $O_3$  concentrations) is typically 4-12 ppbv and only rarely exceeds 20 ppbv (< 1% total incidences). The stratospheric contribution (dotted dark blue line) is always less than 20 ppbv and usually below 10 ppbv. Time series for specific sites are presented below.

## 6. Case Studies: Influence of the Background on Elevated $O_3$ Events in Spring

In this section, we examine the origin of  $O_3$  concentrations observed at three locations where high- $O_3$  events were previously attributed to natural processes: Voyageurs National Park (NP), Minnesota in June; Haywood County, North Carolina in April and May; and Yellowstone NP, Wyoming in March through May. We use observations from CASTNet stations in conjunction with our model simulations to deconstruct the observed concentrations into anthropogenic and natural contributions. Although the model does not always reproduce the peak amplitude of the observations (shown below), its ability to capture the general features in the time series lends confidence to its utility in interpreting the origin of high- $O_3$  events.

At Voyageurs NP in 2001,  $O_3$  concentrations  $\geq 60$  ppbv occurred frequently in June but rarely later in summer (Table 3). A similar pattern was observed in 1995 and 1997 and was used to argue that photochemical activity was probably not responsible for these events [Lefohn *et al.* 2001]. Figure 4 shows that GEOS-CHEM captures much of the day-to-day variability in observed concentrations from mid-May through June, including the occurrence and magnitude of high- $O_3$  events. The simulated background contribution (green diamonds) ranges from 15-36 ppbv with a 25 ppbv mean. The natural  $O_3$  level (blue crosses) is 15 ppbv on average and varies

from 9 to 23 ppbv. The stratospheric contribution (blue X's) is always  $< 7$  ppbv. The dominant contribution to the high- $O_3$  events on June 26 and 29 is from regional pollution (44 and 50 ppbv on June 26 and 29, respectively, calculated as the difference between the red and green lines in Figure 4). The background contribution (green diamonds) is  $< 30$  ppbv on both days, and is composed of a 20 ppbv natural contribution (which includes 2 ppbv of stratospheric origin) and a 5 ppbv enhancement from hemispheric pollution (the difference between the green and light blue lines). Beyond these two high- $O_3$  events, we see from Figure 4 that regional pollution drives most of the simulated day-to-day variability and explains all events above 50 ppbv. In 2001, monthly mean observed and simulated  $O_3$  concentrations are lower in July (37 and 42 ppbv, respectively) and August (35 and 36 ppbv) than in June (44 and 45 ppbv). Inspection of model results leads us to hypothesize that the lower mean  $O_3$  and lack of  $O_3 > 60$  ppbv in July and August reflects a stronger Bermuda High Pressure system that sweeps pollution from southern regions eastward before it can reach Voyageurs NP.

High  $O_3$  ( $> 80$  ppbv) was observed in Haywood County, North Carolina on May 1, 2000 and was attributed by A.S.L. & Associates to stratospheric  $O_3$  reaching the surface on the basis of subsiding isentropic back trajectories and satellite water vapor imagery [<http://www.asl-associates.com/ncreport.htm>]. This event has received attention by EPA regulators because it was the fourth time in that year when  $O_3$  concentrations at the Haywood County monitoring site exceeded the national  $O_3$  standard. Figure 5 shows 13-17 LT observations and model results for Coweeta, NC, the CASTNet site closest to the Haywood County monitor. The observed concentration is 85 ppbv for the May 1 event, and the model gives an excellent simulation of this event (81 ppbv), which includes a 60 ppbv contribution from  $O_3$  produced in the continental lower troposphere. The model can thus explain the Haywood County event on the basis of regional pollution, without enhanced transport from the stratosphere. The bottom panel of Figure 5 shows that all high- $O_3$  events in April-May 2001 can be similarly explained by regional pollution.

Why is there such a difference in interpretation between our analysis and that of A.S.L. & Associates? The latter interpretation was principally based upon the occurrence of subsiding back-trajectories. We first examine whether the GEOS-CHEM fields predict subsidence over this region on May 1, 2000 by calculating back-trajectories with the NASA Langley 3-D trajectory model [*Pierce and Fairlie, 1993; Pierce et al., 1994*] using the GEOS-CHEM fields

interpolated to potential temperature ( $\theta$ ) surfaces [Li *et al.*, 2002a]. Figure 6 shows that the GEOS-CHEM fields exhibit strong subsidence along  $\theta = 300$  K from  $\sim 650$  hPa, consistent with the trajectories posted at [<http://www.asl-associates.com/ncreport.htm>] and used to infer a stratospheric influence. The back-trajectories are thus diagnosing a free-tropospheric origin for the observed air. Free-tropospheric  $O_3$  is not predominantly of stratospheric origin, nor is it all natural; it is mostly controlled by production within the troposphere and includes a major anthropogenic enhancement [e.g. Berntsen *et al.*, 1997; Roelofs *et al.*, 1997; Wild and Akimoto, 2001]. In addition, subsiding back trajectories do not necessarily imply a free-tropospheric origin for  $O_3$  observed at the surface, since the subsiding conditions are also associated with strong inversions and clear skies that promote  $O_3$  production in the continental boundary layer. Indeed, Dickerson *et al.* [1995] and Li *et al.* [2002a] previously showed that high- $O_3$  events observed at Bermuda in spring behind cold fronts can be explained by post-frontal boundary layer outflow of U.S. pollution (see Cooper *et al.* [2002] for a description of the conceptual model), even as back trajectories diagnose the strong subsidence of air behind the front. Cooper *et al.* [1998] showed that while stratospheric intrusions enhance  $O_3$  in the middle and upper troposphere during post-frontal events over the eastern United States in spring, they do not typically extend below 3 km. Finally, in both 2000 and 2001, high  $O_3$  concentrations are associated with warmer temperatures (not shown); the surface air temperature was 26 °C in North Carolina on May 1, 2000. Cooper and Moody [2000] have previously shown that the high  $O_3$  concentrations at an elevated, regionally representative site in the eastern United States in spring coincide with high temperatures and anticyclonic circulation, conditions conducive to photochemical  $O_3$  production.

Frequently observed concentrations of  $O_3$  between 60-80 ppbv at Yellowstone NP in spring have been attributed to natural sources because they occur before local park traffic starts and back-trajectories do not suggest influence from long-range transport of anthropogenic sources [Lefohn, 1997; Lefohn *et al.*, 2001]. More hours with  $O_3 \geq 60$  ppbv occur in April and May of 2001 (Table 2) than in the years analyzed by Lefohn *et al.* [2001]. We use GEOS-CHEM to interpret these events; results are shown in Figure 7. The mean background, natural, and stratospheric  $O_3$  contributions in March-May are higher at Yellowstone, 38, 22, and 8 ppbv, respectively, as compared to 27, 18, and 5 ppbv at the two eastern sites previously discussed. The larger stratospheric contribution at Yellowstone reflects the high elevation of the site (2.5

km). If we were to assume that the model is not properly capturing stratospheric influence at the surface and that this shortcoming explains the entire GEOS-CHEM (red triangles) underestimate of the observed O<sub>3</sub> concentrations (black asterisks) in Figure 7, then we could calculate an upper limit on the stratospheric contribution to the observed total O<sub>3</sub>. Under this assumption, we find 7, 15, and 14 days when afternoon average background concentrations exceed 45 ppbv in March, April, and May of 2001, with upper limits in May of 58, 40, and 25 ppbv, for the background, natural, and stratospheric O<sub>3</sub> levels, respectively. We point out that the natural O<sub>3</sub> level is always < 40 ppbv and argue that the background at Yellowstone NP should be considered an upper limit for U.S. concentrations because of its high elevation. While Yellowstone receives a higher background concentration than the eastern sites, the model shows that regional pollution from North American anthropogenic emissions (difference between the red and green lines) contributes an additional 10-20 ppbv to the highest observed concentrations in April and May. One should not assume that regional photochemistry is inactive in spring, especially considering that UV radiation levels are in fact comparable to those in summer.

We expect higher-altitude western sites to be more frequent recipients of subsidence events that transport high concentrations of O<sub>3</sub> from the free troposphere to the surface. *Cooper and Moody* [2000] cautioned that observations from elevated sites are not generally representative of lower-altitude sites. At Yellowstone, the background O<sub>3</sub> rarely exceeds 40 ppbv, but it is even lower in the east. We illustrate this point in Figure 8 with time series at representative western and southeastern CASTNet sites for the month of March, when the relative contribution of the background should be high. At the western sites, the background is often near 40 ppbv but total surface O<sub>3</sub> concentrations are rarely above 60 ppbv. While variations in the background play a role in governing the observed total O<sub>3</sub> variability at these sites, regional pollution also contributes. Background concentrations are lower (often < 30 ppbv) in the southeastern states where regional photochemical production drives much of the observed variability. Peak O<sub>3</sub> concentrations in this region are associated with lower background concentrations because of chemical and depositional loss during stagnant meteorological conditions that suppress mixing between the boundary layer and the free troposphere [*Fiore et al.*, 2002a].

## **7. Background O<sub>3</sub> for Risk Assessment**

In this section, we derive our best estimates for the O<sub>3</sub> background in the United States for use in risk assessment calculations. We first classify the CASTNet sites (Figure 1) into surface sites (generally below 1.5 km) and elevated sites (above 1.5 km). All elevated sites are in the west. We then aggregate our results to construct the cumulative probability distributions shown in Figure 9, for the 58 surface sites and the 12 elevated sites (Figure 1), and for the three seasons. Mean background at the surface sites in spring is 27 ppbv as compared to 23 ppbv in summer and fall. At these sites, the background is highest for O<sub>3</sub> concentrations near the center of the distribution, and decline as total surface O<sub>3</sub> concentrations increase, for reasons summarized above [Fiore *et al.*, 2002a]. At the elevated sites, the mean background is 36 ppbv in spring versus 30 ppbv in the other seasons. Background concentrations in the fall resemble those in summer but show less variability and do not exceed 40 ppbv anywhere.

We conclude from the above discussion that an appropriate background for use in risk assessments should vary as a function of season, altitude, and total O<sub>3</sub> level. The green diamonds in Figure 9 can be applied for this purpose. In particular, the depletion of the background during high-O<sub>3</sub> events should be taken into account; the current 25-45 ppbv range used by the EPA will underestimate the risk posed by O<sub>3</sub> concentrations above the background under these circumstances. We emphasize that the model is able to reproduce the overall frequency distributions in Figure 9 without a substantial stratospheric contribution to surface O<sub>3</sub>. In particular, the highest observed O<sub>3</sub> concentrations in all seasons and at all altitudes are associated with regional pollution, rather than stratospheric influence. The background O<sub>3</sub> estimates for risk assessment calculations as shown in Figure 9 include the contribution from hemispheric pollution and would be even lower if international emission controls on NO<sub>x</sub> and CH<sub>4</sub> [Fiore *et al.*, 2002b] could be considered as part of a broader strategy to improve U.S. air quality.

## 8. Summary and Conclusions

The EPA defines background O<sub>3</sub> for risk assessment as those concentrations that would exist in the absence of North American anthropogenic emissions. The presently assumed background range of 25-45 ppbv was instrumental in defining the current 84 ppbv national air quality standard (NAAQS). Recent reports of high-O<sub>3</sub> events at remote sites have been used to imply that the natural background could be much higher and that the NAAQS is unachievable.

We investigated the factors responsible for these high-O<sub>3</sub> events and conducted a more general quantitative analysis of the background as a function of season, site location, and local O<sub>3</sub> concentration. We also examined the anthropogenic vs. natural contributions to the background, and the prospects for lowering the background through international control of emissions.

Our approach was to use a CTM to trace the origin of high-O<sub>3</sub> events observed at rural U.S. sites. Sensitivity simulations were conducted to quantify background O<sub>3</sub> and to isolate the contributions from natural sources (including the stratosphere) versus anthropogenic sources outside North America (including CH<sub>4</sub>). The model was shown to simulate much of the day-to-day variability observed at rural U.S. surface sites including high-O<sub>3</sub> events in spring and summer, lending confidence to its utility for source attribution. Previous applications of the model have demonstrated that it simulates the tropospheric ozonesonde climatology [Logan, 1999] generally to within 5-10 ppbv, including at mid and high latitudes, and reproduces the correct seasonal cycle to within 1-2 months [Bey *et al.*, 2001a; Li *et al.*, 2002a; Liu *et al.*, 2002]. The model thus offers an adequate simulation of O<sub>3</sub> in the free troposphere at northern midlatitudes, including the influence from the stratosphere.

We find that the frequently observed elevated O<sub>3</sub> concentrations (50-80 ppbv) at northwestern U.S. surface sites in spring, previously attributed to natural causes such as stratospheric intrusions reaching the surface [Lefohn, 1997; Lefohn *et al.*, 2001], can in fact be primarily explained by O<sub>3</sub> produced from North American anthropogenic emissions. As such they do not represent “direct measurements” of the background. High-elevation sites (> 2 km) occasionally experience high background in spring due to free-tropospheric influence; however this free-tropospheric influence includes a significant contribution from hemispheric pollution (typically 4-12 ppbv), and in any case these sites cannot be viewed as representative of surface air [Cooper and Moody, 2000], where the background is consistently lower. We find that the stratospheric contribution to surface O<sub>3</sub> is of minor importance in the model, always below 20 ppbv.

Previous interpretations of the high-O<sub>3</sub> events in spring were based upon the assumption that strongly subsiding isentropic back trajectories indicate a stratospheric origin. Subsiding conditions diagnosed with these trajectories are also associated with strong inversions and clear skies that promote O<sub>3</sub> production in the continental boundary layer. Furthermore, the subsiding air is not necessarily from the stratosphere; it is well established that most O<sub>3</sub> in the free

troposphere is produced within the troposphere and is greatly enhanced by anthropogenic emissions, at least at northern midlatitudes [e.g. *Berntsen et al.*, 1997; *Roelofs et al.*, 1997; *Wild and Akimoto*, 2001]. Surface O<sub>3</sub> concentrations in excess of the current 84 ppbv national O<sub>3</sub> standard might conceivably occur when stratospheric intrusions reach the surface. However, considering that the model simulates the observed variability of O<sub>3</sub> including the high-O<sub>3</sub> events, we can assert with confidence that these events must be extremely rare. The present formulation of the standard (the fourth highest concentration in excess of 84 ppbv for a three-year averaging period) should adequately screen out such anomalous events. Indeed, *Logan* [1989] analyzed O<sub>3</sub> data over the eastern United States from 1978 and 1979 and found only one surface intrusion, which was clearly marked by cold temperatures and high O<sub>3</sub> in March. More recently, *Cooper et al.* [1998] analyzed daily ozonesonde data from March 22 to May 3, 1996 at two sites in the eastern United States and found that stratospheric intrusions over the eastern United States in spring do not typically reach below 3 km.

The O<sub>3</sub> background in the model is generally 15-35 ppbv, with occasional incidences of 40-50 ppbv at high altitude western sites in spring. It declines from the spring to the summer months and is often less than 25 ppbv under the conditions conducive to high-O<sub>3</sub> episodes. We conclude that the 40 ppbv background currently used by EPA actually underestimates the risk associated with O<sub>3</sub> at polluted sites in summer. The variations in background with season, altitude, and total surface O<sub>3</sub> concentration shown in Figure 9 should be included in the EPA risk assessments.

Although background concentrations are not found to compromise the current 84 ppbv U.S. air quality standard, they do occasionally exceed 40 ppbv. In Europe, a cumulative indicator of O<sub>3</sub> exposure above a 40 ppbv threshold (AOT40) is used as a standard to protect crops and natural vegetation [*Mauzerall and Wang*, 2001]. We show with the model that the natural O<sub>3</sub> level never exceeds 40 ppbv over the United States. Hemispheric pollution, produced from global anthropogenic emissions of NO<sub>x</sub> and CH<sub>4</sub>, occasionally elevates background O<sub>3</sub> in the United States above the 40 ppbv threshold. Meeting an AOT40 type of standard in the United States would thus be facilitated by international efforts to reduce hemispheric pollution.

## Acknowledgments



We thank Dave McKee and Joe Pinto at U.S. EPA for helpful conversations. This work was supported by the EPA Office of Air Quality Planning and Standards (OAQPS) under the Intercontinental Transport and Climatic Effects of Air Pollutants (ICAP) program.

## References

- Altshuller, A.P. and A.S. Lefohn, Background ozone in the planetary boundary layer over the United States, *J. Air & Waste Manage. Assoc.*, **46**, 134-141, 1996.
- Berntsen, T.K., I.S.A. Isaksen, G. Myhre, J.S. Fuglestad, F. Stordal, T.A. Larsen, R.S. Freckleton, and K.P. Shine, Effects of anthropogenic emissions on tropospheric ozone and its radiative forcing, *J. Geophys. Res.*, **102**, 28,101-28,126, 1997.
- Bey, I., D.J. Jacob, R.M. Yantosca, J.A. Logan, B. Field, A.M. Fiore, Q. Li, H. Liu, L.J. Mickley, and M. Schultz, Global modeling of tropospheric chemistry with assimilated meteorology: Model description and evaluation, *J. Geophys. Res.*, **106**, 23,073-23,096, 2001a.
- Bey, I., D.J. Jacob, J.A. Logan, and R.M. Yantosca, Asian chemical outflow to the Pacific in spring: Origins, pathways, and budgets, *J. Geophys. Res.*, **106**, 23,097-23,113, 2001b.
- Cooper, O.R., and J.L. Moody, Meteorological controls on ozone at an elevated eastern United States regional background monitoring site, *J. Geophys. Res.*, **105**, 6855-6869, 2000.
- Cooper, O.R., J.L. Moody, J.C. Davenport, S.J. Otmans, B.J. Johnson, X. Chen, P.B. Shepson, and J.T. Merrill, Influence of springtime weather systems on vertical ozone distributions over three North American sites, *J. Geophys. Res.*, **103**, 22,001-22,013, 1998.
- Cooper, O.R., J.L. Moody, D.D. Parrish, M. Trainer, T.B. Ryerson, J.S. Holloway, G. Hubler, F.C. Fehsenfeld, M.J. Evans, Trace gas composition of midlatitude cyclones over the western North Atlantic Ocean: A conceptual model, *J. Geophys. Res.*, **107** (D7), doi:10.1029/2001JD000901, 2002.
- Dickerson, R.R., B.G. Doddridge, P. Kelley, and K.P. Rhoads, Large-scale pollution of the atmosphere over the remote Atlantic Ocean: Evidence from Bermuda, *J. Geophys. Res.*, **100**, 8945-8952, 1995.
- Duncan, B.N., J.A. Logan, I. Bey, R.V. Martin, D.J. Jacob, R.M. Yantosca, P.C. Novelli, N.B. Jones, and C.P. Rinsland, Model study of variability and trends of carbon monoxide (1988-1997) 1. Model formulation, evaluation, and sensitivity, manuscript in preparation, 2003.
- Evans, M.J., *et al.*, Emissions, evolution and impact of Asian oxides of nitrogen on the regional and global atmosphere, manuscript in preparation, 2003.

- Fiore, A.M., D.J. Jacob, I. Bey, R.M. Yantosca, B.D. Field, A.C. Fusco, and J.G. Wilkinson, Background ozone over the United States in summer: Origin, trend, and contribution to pollution episodes, *J. Geophys. Res.*, *107* (D15), doi:10.1029/2001JD000982, 2002a.
- Fiore, A.M., D.J. Jacob, B.D. Field, D.G. Streets, S.D. Fernandes, and C. Jang, Linking ozone pollution with climate change: The case for controlling methane, *Geophys. Res. Lett.*, *29*, (19), 1919, doi:10.1029/2002GL015601, 2002b.
- Fiore, A.M., D.J. Jacob, R. Mathur, and R.V. Martin, Application of empirical orthogonal functions to evaluate ozone simulations for the eastern United States with regional and global models, in press, *J. Geophys. Res.*, 2003.
- Fusco, A.C. and J.A. Logan, Analysis of 1970-1995 trends in tropospheric ozone at Northern Hemisphere midlatitudes with the GEOS-CHEM model, *J. Geophys. Res.*, in press, 2003.
- Hirsch, A.I., J.W. Munger, D.J. Jacob, L.W. Horowitz, and A.H. Goldstein, Seasonal variation of the ozone production efficiency per unit NO<sub>x</sub> at Harvard Forest, Massachusetts, *J. Geophys. Res.*, *101*, 12,659-12,666, 1996.
- Holton, J.R., P.H. Haynes, M.E. McIntyre, A.R. Douglass, R.B. Rood, and L. Pfister, Stratosphere-Troposphere Exchange, *Rev. Geophys.*, *33*, 403-439, 1995.
- Kasibhatla, P., H. Levy II, A. Klonecki, and W.L. Chameides, Three-dimensional view of the large-scale tropospheric ozone distribution over the North Atlantic Ocean during summer, *J. Geophys. Res.*, *101*, 29,305-29,316, 1996.
- Lavery, T.F., C.M. Rogers, H. Kemp Howell, M.C. Burnett, C.A. Wanta, Clean Air Status and Trends Network (CASTNet) 2000 Annual Report, 2002.  
(available at <http://www.epa.gov/castnet/library/annual00.html>)
- Lefohn, A.S., A new ozone standard in the United States, *Atmos. Environ.*, *31*, 3851-3852, 1997.
- Lefohn, A.S., D.S. Shadwick, and S.D. Ziman, The difficult challenge of attaining EPA's new ozone standard, *Environ. Sci. & Technol.*, *32*, 276A-282A, 1998.
- Lefohn, A.S., S.J. Oltmans, T. Dann, and H.B. Singh, Present-day variability of background ozone in the lower troposphere, *J. Geophys. Res.*, *106*, 9945-9958, 2001.
- Li, Q., D.J. Jacob, J.A. Logan, I. Bey, R.M. Yantosca, H. Liu, R.V. Martin, A.M. Fiore, B.D. Field, and B.N. Duncan, A tropospheric ozone maximum over the Middle East, *Geophys. Res. Lett.*, *28*, 3235-3238, 2001.
- Li, Q., D.J. Jacob, T.D. Fairlie, H. Liu, R.M. Yantosca, and R.V. Martin, Stratospheric versus pollution influences on ozone at Bermuda: Reconciling past analyses, *J. Geophys. Res.*, *107*(D22), 4611, doi:10.1029/2002JD00213, 2002a.

- Li, Q., D.J. Jacob, I. Bey, P.I. Palmer, B.N. Duncan, B.D. Field, R.V. Martin, A.M. Fiore, R.M. Yantosca, D.D. Parrish, P.G. Simmonds, and S.J. Oltmans, Transatlantic transport of pollution and its effects on surface ozone in Europe and North America, *J. Geophys. Res.*, *107*(D13), doi:10.1029/2001JD001422, 2002b.
- Li, Q., *et al.*, Export of NO<sub>y</sub> from the North American boundary layer: Reconciling aircraft observations and global model budgets, manuscript in preparation, 2003.
- Liang, J., L.W. Horowitz, D.J. Jacob, Y. Wang, A.M. Fiore, J.A. Logan, G.M. Gardner, and J.W. Munger, Seasonal variations of reactive nitrogen species and ozone over the United States, and export fluxes to the global atmosphere, *J. Geophys. Res.*, *103*, 13,435-13,450, 1998.
- Lin, C.Y., D.J. Jacob, J.W. Munger, and A.M. Fiore, Increasing background ozone in surface air over the United States, *Geophys. Res. Lett.*, *27*, 3465-3468, 2000.
- Liu, H., D.J. Jacob, L.Y. Chan, S.J. Oltmans, I. Bey, R.M. Yantosca, J.M. Harris, B.N. Duncan, and R.V. Martin, Sources of tropospheric ozone along the Asian Pacific Rim: An analysis of ozonesonde observations, *J. Geophys. Res.*, *107*(D21), 4573, doi: 10.1029/2001JD002005, 2002.
- Liu, H., D.J. Jacob, J.E. Dibb, A.M. Fiore, R.M. Yantosca, Constraints on the sources of tropospheric ozone from <sup>210</sup>Pb-<sup>7</sup>Be-O<sub>3</sub> correlations, *J. Geophys. Res.*, submitted, 2003a.
- Liu, H., D.J. Jacob, I. Bey, R.M. Yantosca, B.N. Duncan, and G.W. Sachse, Transport pathways for Asian pollution outflow over the Pacific: Interannual and seasonal variations, *J. Geophys. Res.*, *108*(D20), 8786, doi: 10.1029/2002JD003102, 2003b.
- Logan, J.A., An analysis of ozonesonde data for the troposphere: Recommendations for testing 3-D models and development of a gridded climatology for tropospheric ozone, *J. Geophys. Res.*, *104*, 16,115-16,149, 1999.
- Logan, J.A., Ozone in Rural Areas of the United States, *J. Geophys. Res.*, *94*, 8511-8532, 1989.
- Marenco, A., H. Gouget, P. Nedelec, J-P Pages, Evidence of a long-term increase in tropospheric ozone from Pic du Midi data series: Consequences: Positive radiative forcing, *J. Geophys. Res.*, *99*, 16,617-16,632, 1994.
- Martin, R.V., D.J. Jacob, K.V. Chance, T.P. Kurosu, P.I. Palmer, and M.J. Evans, Global inventory of nitrogen oxide emissions constrained by space-based observations of NO<sub>2</sub> columns, *J. Geophys. Res.*, *108*(D17), 4537, doi: 10.1029/2003JD003453, 2003.
- Mauzerall, D.L. and Wang, X., Protecting agricultural crops from the effects of tropospheric ozone exposure: Reconciling science and standard setting in the United States, Europe and Asia, *Annual Review of Energy and the Environment*, *26*, 237-268, 2001.

- McDonnell, W.F., K.E. Muller, P.A. Bromberg, and C.M. Shy, Predictors of individual differences in acute response to ozone exposure, *Am. Rev. Respir. Dis.*, 147, 818-825, 1993.
- McLinden, C.A., S.C. Olsen, B. Hannegan, O. Wild, M.J. Prather, and J. Sundet, Stratospheric ozone in 3-D models: A simple chemistry and the cross-tropopause flux, *J. Geophys. Res.*, 105, 14,653-14,665, 2000.
- Odman, M.T., and C.I. Ingram, Multiscale Air Quality Simulation Platform (MAQSIP): Source code documentation and validation, *Tech. Rep. ENV-96TR002-v1.0*, 83 pp., MCNC, Research Triangle Park, North Carolina, 1996.
- Palmer, P.I., D.J. Jacob, K. Chance, R.V. Martin, R.J.D. Spurr, T.P. Kurosu, I. Bey, R. Yantosca, A. Fiore, and Q. Li, Air mass factor formulation for spectroscopic measurements from satellites: Application to formaldehyde retrievals from the Global Ozone Monitoring Experiment, *J. Geophys. Res.*, 106, 14,539-14,550, 2001.
- Palmer, P.I., D.J. Jacob, A.M. Fiore, R.V. Martin, K. Chance, T.P. Kurosu, Mapping isoprene emissions over North America using formaldehyde column observations from space, *J. Geophys. Res.*, 108(D6), doi: 10.1029/2002JD002153, 2003.
- Park, R.J., D.J. Jacob, M. Chin and R.V. Martin, Sources of carbonaceous aerosols over the United States and implications for natural visibility, *J. Geophys. Res.*, 108(D12), 4355, doi: 10.1029/2002JD003190, 2003.
- Pierce, R.B., and T.D. Fairlie, Chaotic advection in the stratosphere: Implications for the dispersal of chemically-perturbed air from the polar vortex, *J. Geophys. Res.*, 98, 18,589-18,595, 1993.
- Pierce, R.B., T.D. Fairlie, W.L. Grose, R. Swinbank, and A. O'Neill, Mixing processes within the polar night jet, *J. Atmos. Sci.*, 51, 2957-2972, 1994.
- Prather M., and D. Ehhalt, Atmospheric chemistry and greenhouse gases, in *Climate Change: The Scientific Basis: The IPCC Working Group I Third Assessment Report*, Cambridge Univ. Press, New York, 2001.
- Roelofs, G-J, J. Lelieveld, and R. van Dorland, A three-dimensional chemistry/general circulation model simulation of anthropogenically derived ozone in the troposphere and its radiative climate forcing, *J. Geophys. Res.*, 102, 23,389-23,401, 1997.
- Trainer M., and 19 others, Correlation of ozone with NO<sub>y</sub> in photochemically aged air, *J. Geophys. Res.*, 98, 2917-2925, 1993.
- United States Environmental Protection Agency (U.S. EPA), Air Quality Criteria for Ozone and Related Photochemical Oxidants, Research Triangle Park, NC, 1996a.

(Available at <http://www.epa.gov/ncea/pdfs/Ozone/Vol1fm.pdf>)

U.S. EPA, Review of National Ambient Air Quality Standards for Ozone, Assessment of Scientific and Technical Information, OAQPS Staff Paper, EPA-452/R-96-007, Research Triangle Park, 1996b.

(Available at [http://www.epa.gov/ttn/naaqs/standards/ozone/s\\_o3\\_pr\\_sp.html](http://www.epa.gov/ttn/naaqs/standards/ozone/s_o3_pr_sp.html))

U.S. EPA, Latest Findings on National Air Quality 2001 Status and Trends, *EPA 454/K-02-001*, Research Triangle Park, NC, 2002.

(Available at <http://www.epa.gov/airprogm/oar/aqtrnd01/summary.pdf>)

U.S. EPA, Air Quality Criteria for Ozone and Related Photochemical Oxidants, Research Triangle Park, NC, manuscript in preparation, 2003.

Wang, Y., D.J. Jacob, and J.A. Logan, Global simulation of tropospheric ozone-NO<sub>x</sub>-hydrocarbon chemistry, 3. Origin of tropospheric ozone and effects of non-methane hydrocarbons, *J. Geophys. Res.*, 103/D9, 10,757-10,768, 1998.

Wild, O., and H. Akimoto, Intercontinental transport of ozone and its precursors in a three-dimensional global CTM, *J. Geophys. Res.*, 106, 27,729-27,744, 2001.

## Figure Captions

**Figure 1.** CASTNet stations in the continental United States for 2001. Sites discussed in section 6 are labeled: VOY=Voyageurs NP, MI; COW=Coweeta, NC; YEL=Yellowstone NP, WY; CAD=Caddo Valley, AR; CVL=Coffeeville, MS; GAS=Georgia Station, GA; GRB=Great Basin, NV; GRC=Grand Canyon, AZ; CAN=Canyonlands, UT; MEV=Mesa Verde, CO. Crosses denote sites above 1.5 km altitude.

**Figure 2.** Monthly mean afternoon (13-17 LT) O<sub>3</sub> concentrations (ppbv) in surface air averaged over the CASTNet stations (Figure 1) in each U.S. quadrant for March-October 2001. Observations (black asterisks) are compared with model values from the standard simulation sampled at the CASTNet sites (red triangles) and sampled for the entire quadrant (red squares). The vertical lines show the standard deviation in the observed (black) and simulated (red) values. Monthly mean model results for the background (green diamonds), natural (light blue crosses), and stratospheric (blue X's) contributions (Table 2) to surface O<sub>3</sub> are shown. Details are given in section 3. The U.S. quadrants are centered at 98.75°W and 37°N.

**Figure 3.** Probability distributions of daily mean afternoon (13-17 LT) O<sub>3</sub> concentrations in surface air for March through October 2001 at U.S. CASTNet sites (Figure 1): observations (thick black line) are compared with model results (thin red line). Additional probability distributions are shown for the simulated background (long-dashed green line), natural (short-dashed light blue line), and stratospheric (dotted blue line) contributions to surface O<sub>3</sub> (Table 2).

**Figure 4.** Daily mean afternoon (13-17 LT) O<sub>3</sub> concentrations in surface air at Voyageurs National Park (NP), Minnesota in mid-May through June of 2001. Observations (black asterisks) are compared with model values from the standard simulation (red triangles). The simulated contributions from background (green diamonds), natural (light blue crosses), and stratospheric (blue X's) O<sub>3</sub> are also shown.

**Figure 5.** Same as for Figure 4, but for April-May 2000 (upper panel) and April-May 2001 (bottom panel) at the Coweeta, North Carolina, CASTNet site (83°W, 35°N). Blue squares in the 2000 simulation denote O<sub>3</sub> produced in the continental boundary layer (surface-700 hPa).

**Figure 6.** Isentropic back-trajectory calculated from the GEOS meteorological fields with the NASA Langley 3-D trajectory model [*Pierce and Fairlie*, 1993; *Pierce et al.*, 1994; *Li et al.*, 2002] at  $\theta = 300$  K for air arriving in North Carolina on May 1, 2000, 0000 UTC. The average trajectory for 25 parcels ending within the area of 33-37°N and 81-85°W is shown, along with the standard deviations for pressure at each 24-hour interval. The parcels are initialized at a 1° x 1° horizontal resolution.

**Figure 7.** Same as Figure 4 but for Yellowstone NP, Wyoming in March-May 2001.

**Figure 8.** Same as Figure 4 but for March of 2001 at selected western (left column) and southeastern (right column) sites. See section 6 for discussion.

**Figure 9.** Best estimate of background contribution to surface afternoon (13-17 LT) O<sub>3</sub> concentrations in the United States as a function of local O<sub>3</sub> concentration, site altitude, and season. The figure shows cumulative probability distributions of O<sub>3</sub> concentrations for the observations (black asterisks) and the model (red triangles). The corresponding distribution of background O<sub>3</sub> concentrations is shown as green diamonds.

Table 1: Previous estimates of background O<sub>3</sub> in surface air over the United States

Study	Method	Time period	Region	Background Estimate (ppbv)
<i>Trainer et al.</i> , 1993	y-intercept of O <sub>3</sub> vs. NO <sub>y</sub> -NO <sub>x</sub> regression line <sup>a</sup>	Summer 1988	Eastern United States	30-40
<i>Hirsch et al.</i> , 1996	y-intercept of O <sub>3</sub> vs. NO <sub>y</sub> -NO <sub>x</sub> regression line	May-Sep 1990-1994	Harvard Forest <sup>b</sup>	25 (Sept) – 40 (May)
<i>Altshuller and Lefohn</i> , 1996	y-intercept of O <sub>3</sub> vs. NO <sub>y</sub> regression line, and observations at remote/rural sites	Apr-Oct 1988-1993	Continental United States	25-45 (inland) 25-35 (coastal)
<i>Liang et al.</i> , 1998	Sensitivity simulation in a 3-D model with anthropogenic NO <sub>x</sub> emissions in the continental U.S. set to zero	Full year	Continental United States	20-30 (east) 20-40 (west) (spring maximum)
<i>Lin et al.</i> , 2000	Median O <sub>3</sub> values for the lowest 25 <sup>th</sup> percentiles of CO and NO <sub>y</sub> concentrations	1990-1998	Harvard Forest	35 (fall)- 45 (spring)
<i>Fiore et al.</i> , 2002a	O <sub>3</sub> produced outside of the North American boundary layer in a global 3-D model	Summer 1995	Continental United States	15-30 (east) 25-35 (west)

<sup>a</sup> NO<sub>y</sub> is the chemical family including NO<sub>x</sub> and its oxidation products; NO<sub>y</sub>-NO<sub>x</sub> denotes the chemically processed component of NO<sub>y</sub>.

<sup>b</sup> rural site in central Massachusetts

Table 2: Description of simulations used for source attribution

Simulation	Description	Horizontal Resolution
Standard	Present-day emissions as described in the text	2° x 2.5°
Background	North American anthropogenic NO <sub>x</sub> , NMVOC and CO emissions set to zero	2° x 2.5°
Natural	Global anthropogenic NO <sub>x</sub> , NMVOC and CO emissions set to zero and CH <sub>4</sub> concentration set to its 700 ppbv pre-industrial value	4° x 5°
Stratospheric	Tagged O <sub>3</sub> tracer originating from the stratosphere in standard simulation	2° x 2.5°

Table 3: Number of hours with O<sub>3</sub> above 50 or 60 ppbv at U.S. CASTNet sites in 2001

Site	Mar	Apr	May	Jun	Jul	Aug	Sep	Oct
<i>Observations <math>\geq 50</math> ppbv</i>								
Denali NP, Alaska (64°N, 149°W, 0.6 km)	24	302	98	6	0	0	0	0
Voyageurs NP, Minnesota (48°N, 93°W, 0.4 km)	0	0	62	95	14	17	33	0
Glacier NP, Montana (49°N, 114°W, 1.0 km)	4	0	23	0	6	12	0	0
Yellowstone NP, Wyoming (45°N, 110°W, 2.5 km)	307	461	350	172	140	261	173	77
All CASTNet sites (71)	5468 (11%)	15814 (32%)	17704 (36%)	16150 (33%)	14489 (29%)	15989 (32%)	9874 (20%)	5642 (11%)
All sites, 13-17 LT only (hourly data)	1817 (21%)	4684 (56%)	5174 (61%)	4624 (56%)	4613 (54%)	5075 (60%)	3343 (40%)	1945 (23%)
All sites, 13-17 LT mean (4-hour average)	435 (20%)	1153 (55%)	1295 (61%)	1147 (55%)	1161 (54%)	1283 (60%)	841 (40%)	478 (22%)
All sites, model 13-17 LT mean	254 (12%)	1249 (59%)	1527 (69%)	1505 (71%)	1475 (67%)	1500 (68%)	1080 (51%)	591 (27%)
<i>Observations <math>\geq 60</math> ppbv</i>								
Denali NP	0	0	9	2	0	0	0	0
Voyageurs NP	0	0	6	32	0	0	15	0
Glacier NP	0	0	0	0	0	0	0	0
Yellowstone NP	4	77	139	18	6	26	1	2
All sites	519 (1%)	4729 (10%)	8181 (16%)	8199 (17%)	5705 (11%)	7407 (15%)	3492 (7%)	2073 (4%)
All sites, 13-17 LT only	235 (3%)	1798 (22%)	2808 (33%)	2721 (33%)	2235 (26%)	2758 (33%)	1416 (17%)	878 (10%)
All sites, 13-17 LT mean	56 (3%)	428 (20%)	697 (33%)	671 (32%)	550 (26%)	677 (32%)	358 (17%)	214 (10%)
All sites, model 13-17 LT mean	13 (1%)	377 (18%)	834 (38%)	964 (45%)	910 (41%)	834 (38%)	502 (24%)	204 (9%)

Data from 71 U.S. CASTNet sites are included in this analysis: those in Figure 1 plus Denali NP. Percentages of total occurrences are shown in parentheses.  
NP = National Park; LT = Local Time.



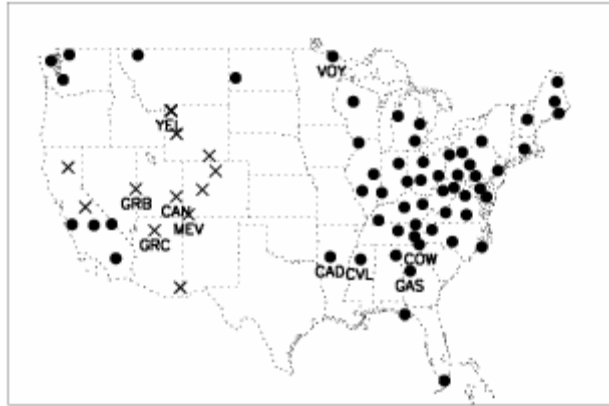


Figure 1.

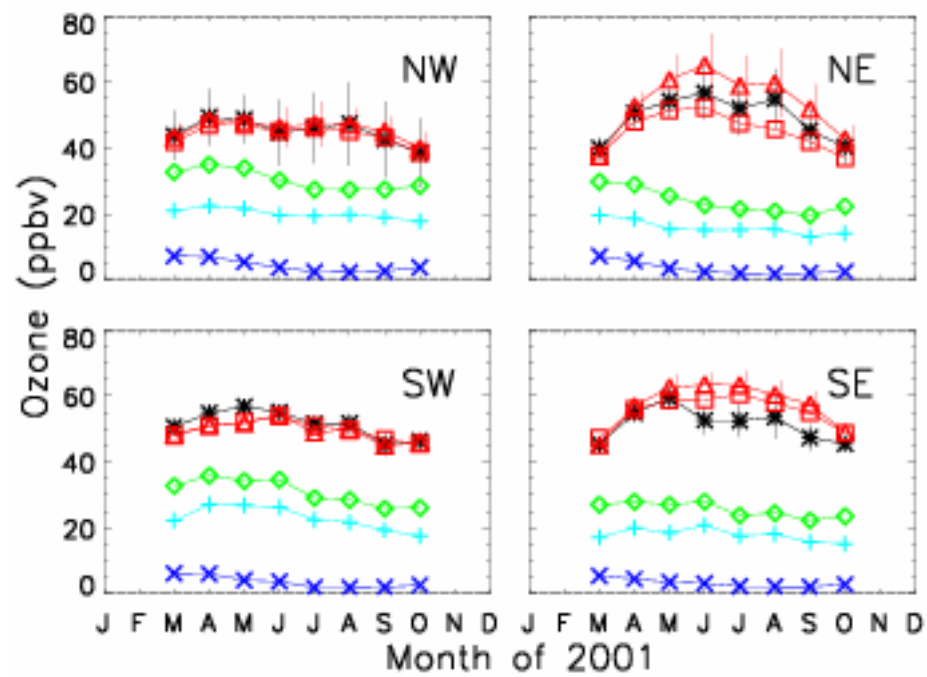


Figure 2.

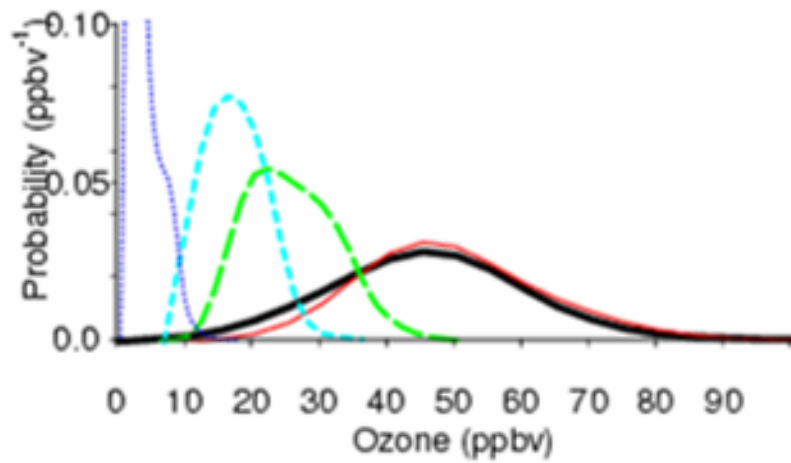


Figure 3.

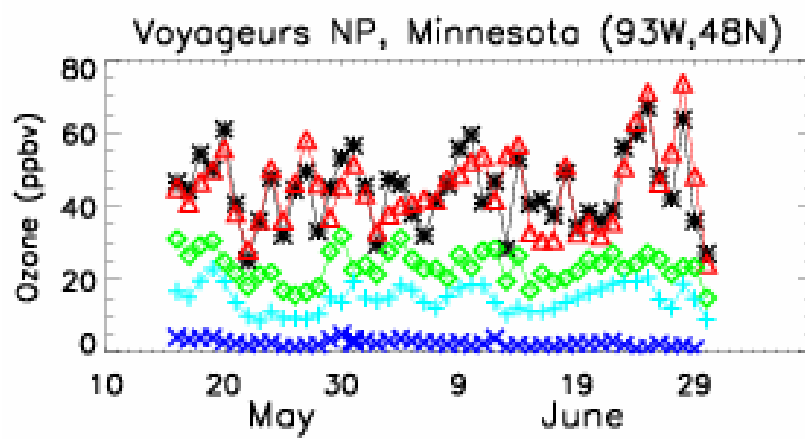


Figure 4.

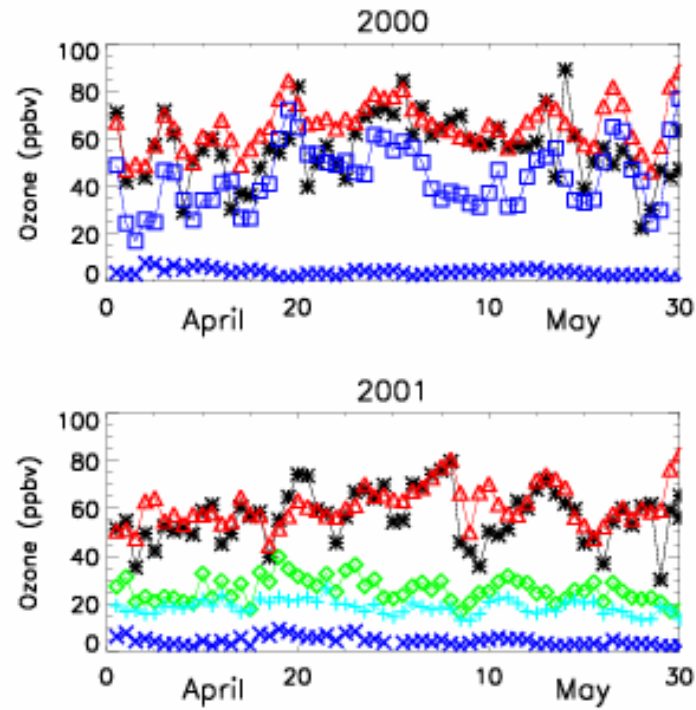


Figure 5.

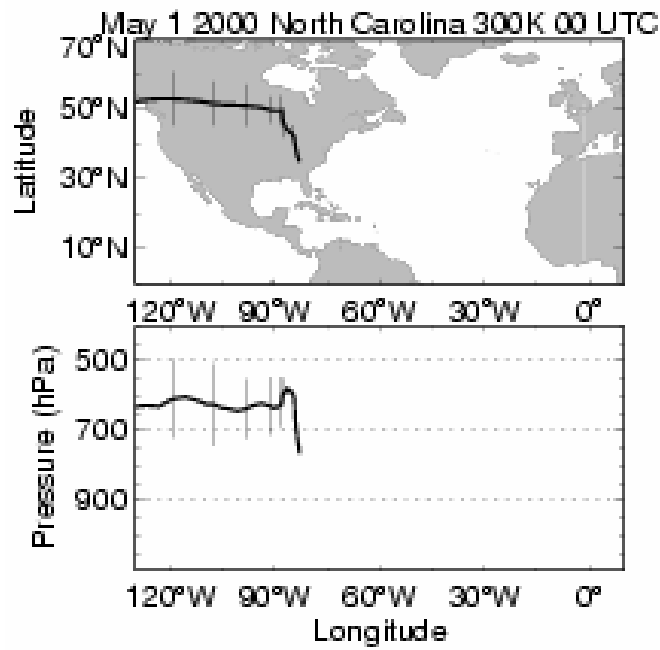


Figure 6.

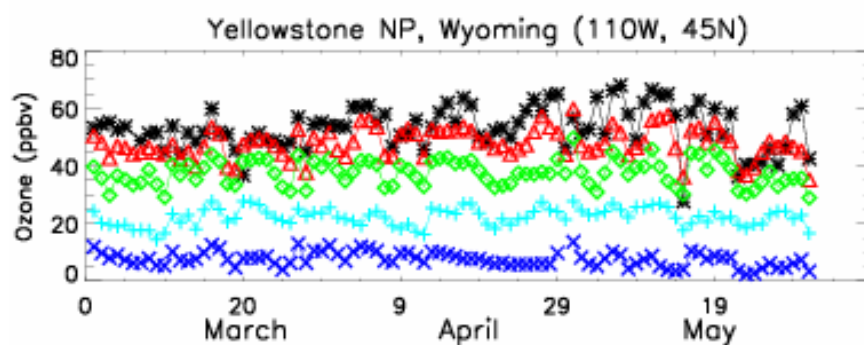


Figure 7.

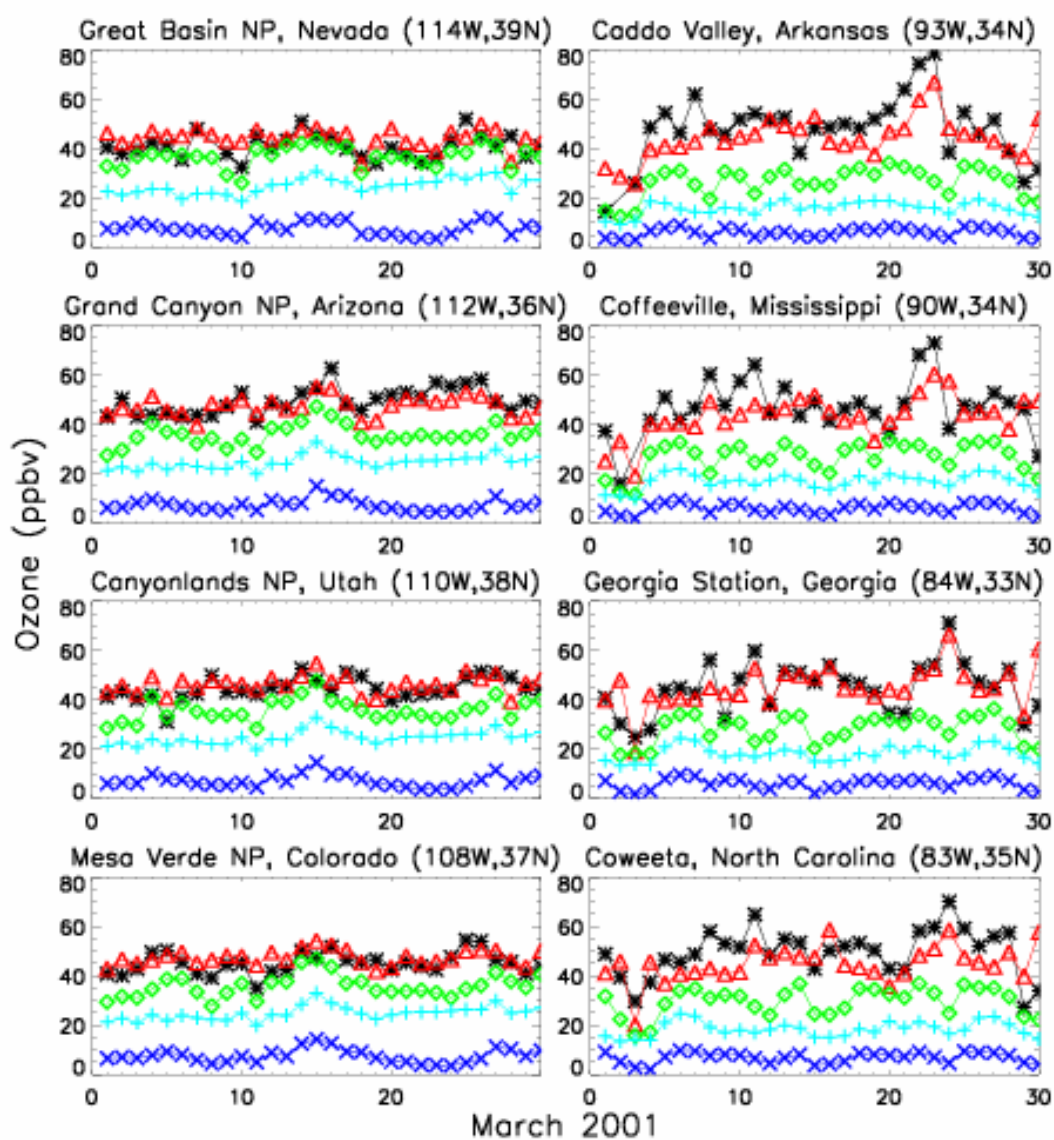


Figure 8.

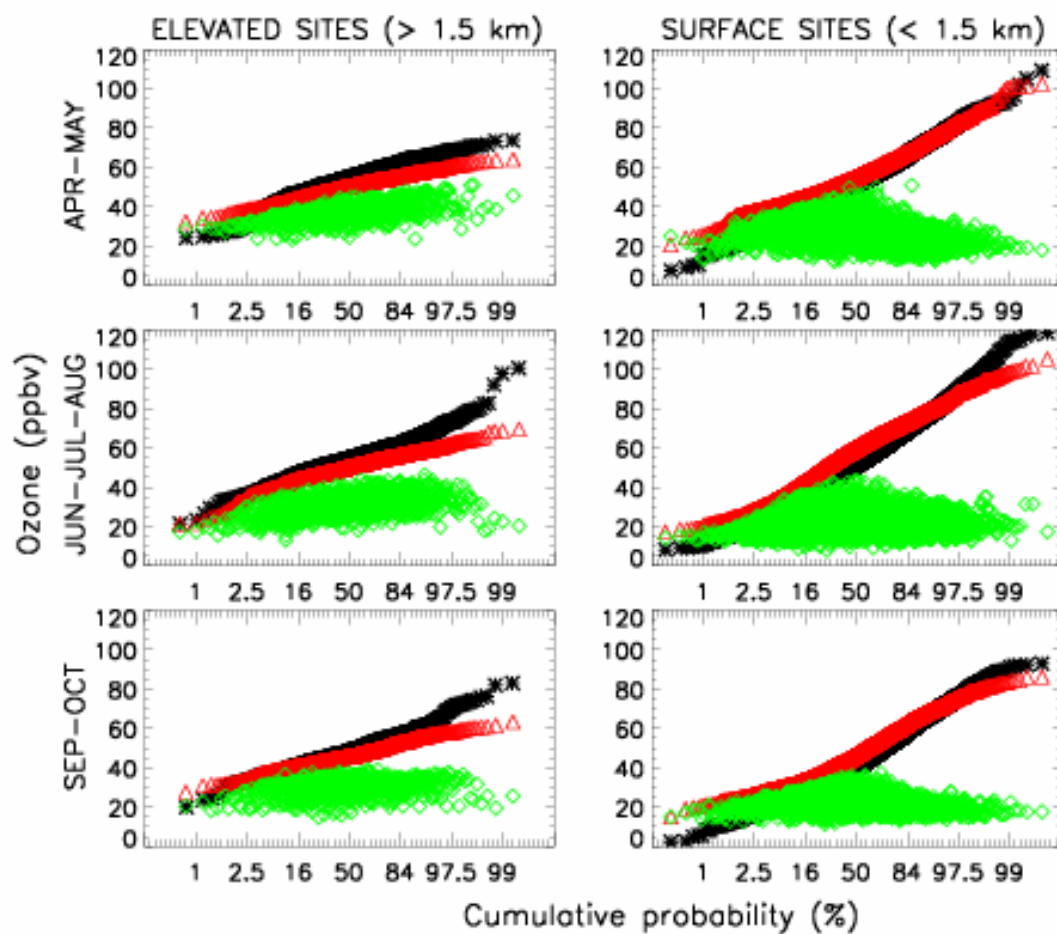


Figure 9.